

# VIBRATIONAL MODE ANALYSIS OF VOID INDUCED CORONENE AS A POSSIBLE CARRIER OF THE ASTRONOMICAL AROMATIC INFRARED BANDS

NORIO OTA

<sup>1</sup> Graduate School of Pure and Applied Sciences, University of Tsukuba,

1-1-1 Tenoudai Tsukuba-city 305-8571, Japan; [n-otajitaku@nifty.com](mailto:n-otajitaku@nifty.com)

Void induced di-cation coronene  $C_{23}H_{12}^{++}$  is a possible carrier of the astronomically observed polycyclic aromatic hydrocarbon (PAH). Based on density functional theory, multiple spin state analysis was done for neutral void coronene  $C_{23}H_{12}$ . Singlet spin state was most stable (lowest total energy). By the Jahn-Teller effect, there occurs serious molecular deformation. Point group D<sub>6h</sub> of pure coronene transformed to C<sub>2</sub> symmetry having carbon two pentagons. Advanced singlet stable molecules were di-cation  $C_{23}H_{12}^{++}$  and di-anion  $C_{23}H_{12}^{--}$ . Molecular configuration was almost similar with neutral  $C_{23}H_{12}$ . However, electric dipole moment of these two charged molecules show reversed direction with 1.19 and 2.63 Debye. Calculated infrared spectrum of  $C_{23}H_{12}^{++}$  show a very likeness to observed one of two astronomical sources of HD44179 and NGC7027. Harmonic vibrational mode analysis was done for  $C_{23}H_{12}^{++}$ . At 3.2  $\mu\text{m}$ , C-H stretching at pentagons was featured. From 6.4 to 8.7 $\mu\text{m}$ , C-C stretching mode was observed. In-plane-bending of C-H was in a range of 7.6-9.2 $\mu\text{m}$ . Both C-H out-of plane bending and C-C stretching were accompanied from 11.4 to 14.3 $\mu\text{m}$ . Astronomically observed emission peaks of 3.3, 6.2, 7.6, 7.8, 8.6, 11.2, 12.7, 13.5 and 14.3 $\mu\text{m}$  were compared well with calculated peaks of 3.2, 6.5, 7.6, 7.8, 8.6, 11.4, 12.9, 13.5, and 14.4 $\mu\text{m}$ .

*Key words* : astrochemistry - infrared: general – methods: numerical – molecular data

Online-only material: color figures

## 1, INTRODUCTION

Interstellar dust show mid-infrared emission from 3 to 20 $\mu\text{m}$ . Discrete emission features at 3.3, 6.2, 7.6, 7.8, 8.6, 11.2, and 12.7 $\mu\text{m}$  are ubiquitous peaks observed at many astronomical objects (Ricca et al. 2012; Geballe et al. 1989; Verstraete et al. 1996; Moutou et al. 1999; Meeus et al. 2001; Peeters et al. 2002; Regan et al. 2004; Engelbracht et al. 2006; Armus et al. 2007; Smith et al. 2007; Sellgren et al. 2007). Current understanding is that these astronomical spectra come from the vibrational modes of polycyclic aromatic hydrocarbon (PAH) molecules. Concerning PAH spectra, there are many experimental (Szczepanski & Vala 1993a; Schlemmer et al. 1994; Moutou et al. 1996; Cook et al. 1998; Piest et al. 1999; Hudgins & Allamandola 1999a, 1999b; Oomens et al. 2001, 2003, 2011; Kim et al. 2001) and density functional theory (DFT) based theoretical analysis (de Frees et al. 1993; Langhoff 1996; Mallocci et al. 2007; Pathak & Rastogi 2007; Bauschlicher et al. 2008, 2009; Ricca et al. 2010, 2011b, 2012).

The current central concept to understand the observed astronomical spectra is the decomposition method from the data base of many PAHs experimental and theoretical analysis (Boersma et al. 2013, 2014). Recently, Tielens (Tielens 2013) discussed void induced graphene like PAH's, which may be candidates of emission source. In a previous paper (Ota 2014b), void induced coronene  $C_{23}H_{12}^{++}$  show a very likeness to well observed one by using DFT calculation

method. The aim of this paper is to analyze molecule harmonic vibration mode of  $C_{23}H_{12}^{++}$ . Also, multiple spin state of void coronene was studied to search serious Jahn-Teller effect resulting characteristic molecular configuration and fairly large electronic dipole.

## 2, CALCULATION METHOD

We have to obtain total energy, optimized atom configuration, and infrared vibrational mode frequency and strength depend on a given initial atomic configuration, charge and spin state Sz. Density functional theory (DFT) with unrestricted B3LYP functional (Becke 1993) was applied utilizing Gaussian09 package (Frisch et al. 2009, 1984) employing an atomic orbital 6-31G basis set. The first step calculation is to obtain the self-consistent energy, optimized atomic configuration and spin density. TR Required convergence on the root mean square density matrix was less than  $10^{-8}$  within 128 cycles. Based on such optimized results, atomic vibrational frequency and strength was calculated. Vibration strength is obtained as molar absorption coefficient  $\epsilon$  (km/mol). Comparing DFT harmonic wavenumber  $N_{\text{DFT}}(\text{cm}^{-1})$  with experimental data, a single scale factor 0.958 was used (Ricca et al. 2012). Observed spectra are astronomical PAHs emission. As noted details by Ricca et al. (Ricca et al. 2012), we should consider photon absorbed emission and apply red shift by  $15 \text{ cm}^{-1}$ .

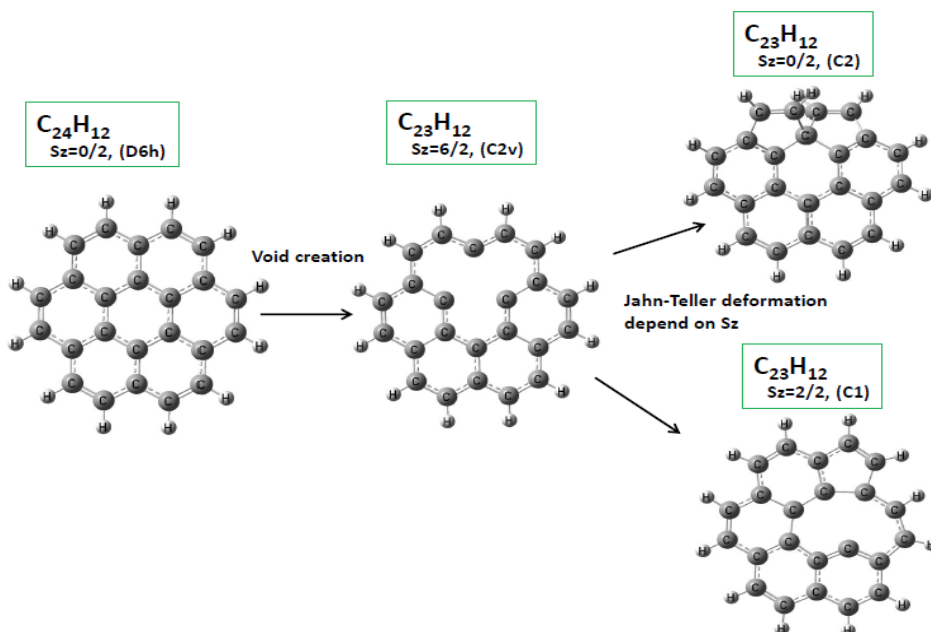


**Figure 1.** Void induced coronene family. Pure coronene has  $D_{6h}$  point group symmetry. Optimized molecular configuration depends on spin state  $S_z$  by the Jahn-Teller effect. Singlet spin state ( $S_z=0/2$ ) of  $C_{23}H_{12}$  show group symmetry  $C_2$  with carbon two pentagons, whereas triplet ( $S_z=2/2$ )  $C_1$  with one pentagon.

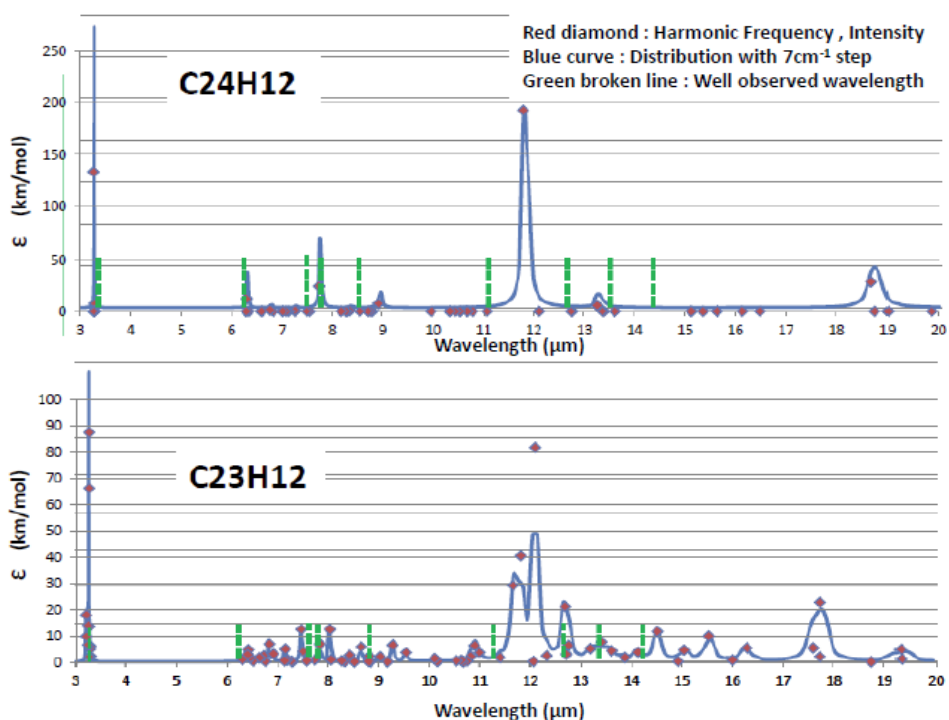


**Figure 2.** Calculated and corrected infrared spectra of  $C_{24}H_{12}$  and singlet spin state  $C_{23}H_{12}$ . Red diamond show harmonic wavelength (micrometer) and intensity epsiron (km/mol). Blue curve is its distribution. Green broken lines are well observed wavelength in interstellar dust.

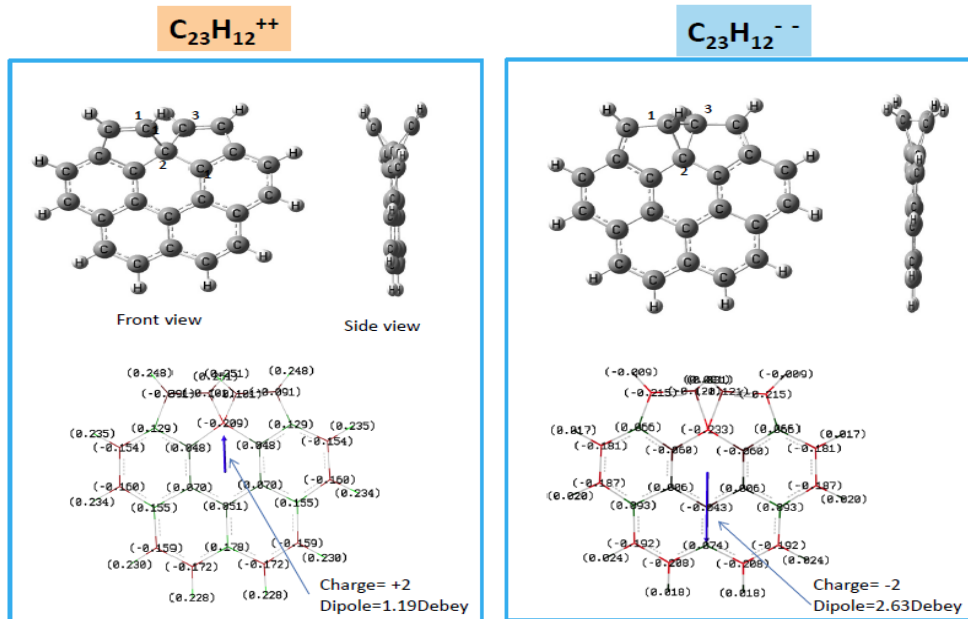


**Figure 3.** Comparing di-cation C<sub>23</sub>H<sub>12</sub><sup>++</sup> with di-anion C<sub>23</sub>H<sub>12</sub><sup>--</sup>, molecular configuration is almost similar with carbon two pentagons. However, electric dipole moment (blue arrow) show reversed direction with 1.19 and 2.63 Debye.

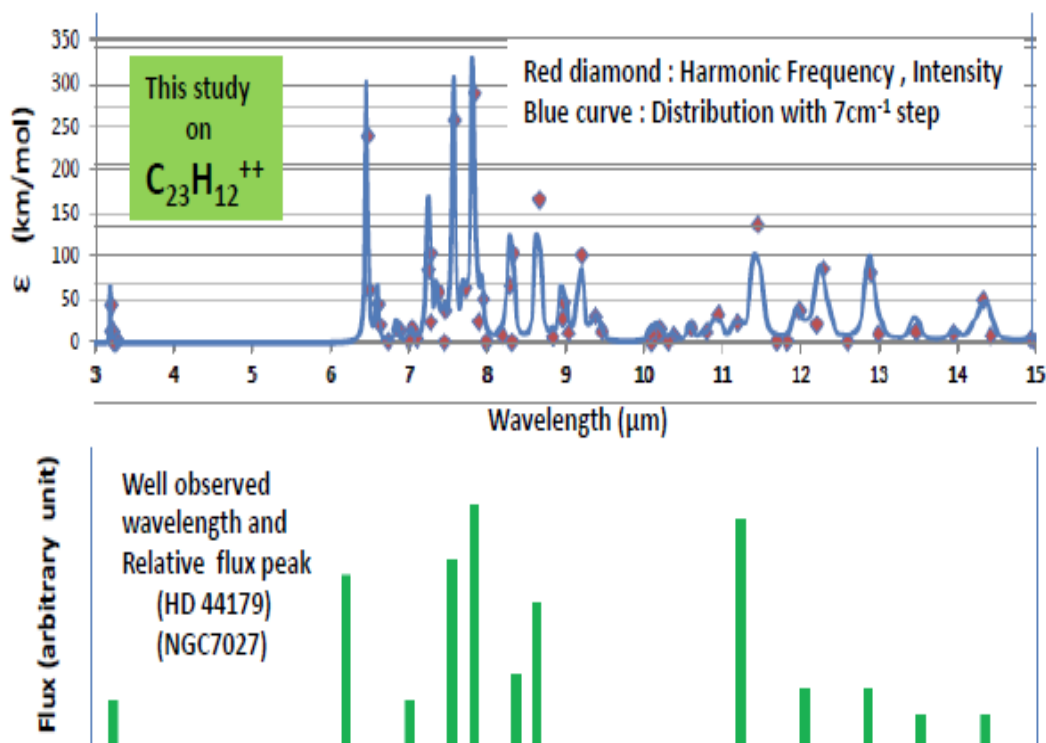


**Figure 4.** Calculated harmonic wavelength and intensity of C<sub>23</sub>H<sub>12</sub><sup>++</sup> is shown by red diamond and their distribution curve by a blue curve based on every 7 cm<sup>-1</sup> accumulation step. Green bar is observed flux peak position and height relatively estimated through two astronomical sources of HD44179 and NGC7027 (modified original spectra; Boersma et al. 2009).

Corrected wave number N is obtained simply by,

$$N(\text{cm}^{-1}) = N_{\text{DFIT}}(\text{cm}^{-1}) \times 0.958 - 15 (\text{cm}^{-1})$$

Also, wavelength  $\lambda$  is,

$$\lambda(\mu\text{m}) = 10000/N(\text{cm}^{-1})$$

In order to compare with reported calculations on pure coronene spectrum, Appendix 1 is inserted in this paper, where wavelength is corrected one.

### 3, MULTIPLE SPIN STATE AND JAHN-TELLER DISTORTION

Void coronene molecules were illustrated in Figure 1. Pure coronene  $\text{C}_{24}\text{H}_{12}$  is non-magnetic ( $S_z=0/2$ ) having D<sub>6h</sub> point group symmetry.

Creation of carbon single void was supposed as shown in middle part of Figure 1 as  $\text{C}_{23}\text{H}_{12}$ . There are six unpaired electrons, which means multiple spin state capability of  $S_z=6/2, 4/2, 2/2$  and  $0/2$ . We should find which one is the most stable (lowest total energy).

Table 1 was a result comparing energy difference between spin state  $S_z$ . Most stable one was singlet state ( $S_z=0/2$ ). Next is triplet ( $S_z=2/2$ ) with 70 kcal/mol higher than singlet. Also, we should compute molecular configuration depend on spin state, that is, such a void brings quantum mechanical distortion by the Jahn-Teller effect (Ota; 2011, 2014a). It is amazing that there cause bond-bond reconstruction. In case of singlet spin state (right upper part in Figure 1), we can see carbon two pentagons connected with five hexagons with a point group symmetry of C<sub>2</sub>. Whereas, in triplet case (lower part), one pentagon was observed with C<sub>1</sub> point group.

**Table 1**

Multiple spin state analysis of neutral void coronene  $\text{C}_{23}\text{H}_{12}$ . By a creation of single carbon void, there brings four spin states. Most stable (lowest total energy) one was  $S_z=0/2$  (singlet). Increasing spin parameter  $S_z$ , total energy increases and became unstable

Input $S_z$	Calculated S(S+1)	Energy difference (kcal/mol)	Molecule Point group
0/2	0.00	0	C <sub>2</sub>
2/2	2.05	70	C <sub>1</sub>
4/2	6.13	130	C <sub>1</sub>
6/2	12.04	208	C <sub>2v</sub>

### 4. Di-CATION $\text{C}_{23}\text{H}_{12}^{++}$ AND Di-ANION $\text{C}_{23}\text{H}_{12}^{--}$

Unfortunately, infrared spectrum of singlet state neutral void coronene  $\text{C}_{23}\text{H}_{12}$  was far from observed one as shown in Figure 2. We should find other candidate. One idea is spin canceling mechanism considering molecular orbits. Advanced singlet spin state molecules will be di-cation  $\text{C}_{23}\text{H}_{12}^{++}$  and di-anion  $\text{C}_{23}\text{H}_{12}^{--}$ . Because, by pulling out two electrons from HOMO level of singlet  $\text{C}_{23}\text{H}_{12}$  we can realize singlet state to be  $\text{C}_{23}\text{H}_{12}^{++}$ . Whereas, by adding two electrons to LUMO level we can realize again singlet state as  $\text{C}_{23}\text{H}_{12}^{--}$ .

Optimized configuration was illustrated in Figure 3, which show similar configuration in both cases, but somewhat detailed discrepancy on two pentagons connected angle C<sub>1</sub>-C<sub>2</sub>-C<sub>3</sub> (see Figure 3 attached number beside carbons). In case of  $\text{C}_{23}\text{H}_{12}^{++}$ , it was 95°, while  $\text{C}_{23}\text{H}_{12}^{--}$  58° which is smaller enough to make an extra sigma bonding between C<sub>1</sub> and C<sub>3</sub>. Important issue is a charge distribution and electric dipole moment. Lower part of Figure 3 show charge distribution by a small letter. In case of  $\text{C}_{23}\text{H}_{12}^{++}$ , hydrogen has plus charge of 0.22e to 0.25e, while  $\text{C}_{23}\text{H}_{12}^{--}$  small value of 0.01e to 0.02e. Electric dipole reflects such distribution. Dipole of  $\text{C}_{23}\text{H}_{12}^{++}$  was 1.19 Debye oriented to upward in a molecule-plane, whereas that of  $\text{C}_{23}\text{H}_{12}^{--}$  was 2.63 Debye downward vector.

### 5, MID-IR SPECTRUM OF $\text{C}_{23}\text{H}_{12}^{++}$

In Figure 4, Calculated harmonic wavelength and intensity of  $\text{C}_{23}\text{H}_{12}^{++}$  is shown by red diamond and their distribution curve by blue accumulating every 7 cm<sup>-1</sup> step. Green bar is observed flux peak position and height relatively estimated through two astronomical sources of HD44179 and NGC7027. Original full observed data was opened by Boersma et al. (Boersma et al 2009). We can see good coincidence between two. Of course, it should be noted that observation is emission flux, while this calculation show absorption. We need advanced calculation on emission using harmonic vibration results appeared in Appendix 2. Detailed data were shown in Table 2. Observed peaks are 3.3, 6.2, 7.6, 7.8, 8.6, 11.2, 12.7, 13.5 and 14.3μm, whereas calculated peaks 3.2, 6.5, 7.3, 7.6, 7.8, 8.3, 8.7, 9.0, 9.2, 11.4, 12.9, 13.5, and 14.3μm respectively. We cannot identify 9.0 and 9.2μm calculated peaks in observed one. Also, we should

notice a large discrepancy at 11.2 $\mu$ m band. Calculated relative intensity is almost one third of observed one.

More inspection and study is necessary to have a complete set of molecules. Anyway, this study could present almost good coincidence by a single molecule  $C_{23}H_{12}^{++}$ .

Concerning di-anion  $C_{23}H_{12}^{--}$ , unfortunately, calculated spectrum (Ota 2014b) was very different with observed one.

**Table 2**

Vibrational mode analysis of  $C_{23}H_{12}^{++}$ . Large intensity modes were selected among full 99 modes noted in appendix 2. Calculated and corrected (scale factor and red shift) wavelength was compared with well observed one in interstellar dust.

Observation	Calculation for $C_{23}H_{12}^{++}$			
Well observed wavelength ( $\mu$ m)	wavelength ( $\mu$ m)	Vibration mode	Harmonic number (Appendix2)	notes
3.3	3.19	C-H stretching at pentagons	98	
6.2	6.46	C-C stretching at hexagons	87	
	7.27	C-C stretching at all carbons	75	Not identified
7.6	7.57	C-H in-plane bending, C-C stretching	71	
7.8	7.82	C-H in-plane bending, C-C stretching	69	
	7.93	C-H in-plane bending, C-C stretching	67	
	8.32	C-H in-plane bending, C-C stretching	62	Uncertain Observation
8.6	8.65	C-H in-plane bending, C-C stretching	61	
	8.97	C-H in-plane bending	58	Not identified
	9.19	C-H in-plane bending	56	Not identified
11.2	11.44	C-H out-of-plane bending, C-C stretching	43	
	12.28	C-H out-of-plane bending, C-C stretching	38	Uncertain
12.7	12.88	C-H out-of-plane bending, C-C stretching	36	
13.5	13.47	C-H out-of-plane bending at pentagons	33	
14.3	14.32	C-H out-of plane bending at pentagons, C-C stretching	31	
17.1	17.09	Carbon out-of-planebending	25	
	22.14	Hexagon in-plane twisting	17	
	31.01	Hexagon in-plane twisting	11	
	56.37	Molecule out-of-plane bending	5	

## Appendix 1. C<sub>24</sub>H<sub>12</sub> fundamental vibrations

C <sub>24</sub> H <sub>12</sub>											
D6h point group symmetry											
Harmonic number	symmetry	Wavelength (μm)	IR Intensity (km/mol)								
1	E <sub>2u</sub>	136.699517	0	31	E <sub>2g</sub>	15.1289339	0	67	A <sub>2g</sub>	8.10510875	0
2	E <sub>2u</sub>	136.699517	0	32	E <sub>2u</sub>	13.6153375	0	68	E <sub>1u</sub>	7.73764214	24.3467
3	A <sub>2u</sub>	91.1560427	5.0256	33	E <sub>2u</sub>	13.6153375	0	69	E <sub>1u</sub>	7.73764214	24.3464
4	B <sub>1g</sub>	67.8436339	0	34	B <sub>1g</sub>	13.3998949	0	70	B <sub>2u</sub>	7.55650469	0
5	B <sub>2g</sub>	47.5113269	0	35	B <sub>2g</sub>	13.3656672	0	71	A <sub>1g</sub>	7.49973040	0
6	E <sub>1g</sub>	36.114981	0	36	E <sub>1u</sub>	13.2604932	5.6576	72	E <sub>2g</sub>	7.26601933	0
7	E <sub>1g</sub>	36.114981	0	37	E <sub>1u</sub>	13.2604932	5.6573	73	E <sub>2g</sub>	7.26601933	0
8	E <sub>2u</sub>	35.3787579	0	38	E <sub>1u</sub>	12.7646716	0.0659	74	E <sub>1u</sub>	7.26303698	0.9008
9	E <sub>2u</sub>	35.3787579	0	39	E <sub>1u</sub>	12.7646716	0.066	75	E <sub>1u</sub>	7.26303698	0.901
10	E <sub>2g</sub>	28.8572000	0	40	E <sub>2u</sub>	12.7436726	0	76	B <sub>1u</sub>	7.13856334	0
11	E <sub>2g</sub>	28.8572000	0	41	E <sub>2u</sub>	12.7436726	0	77	E <sub>2g</sub>	7.09505964	0
12	E <sub>1u</sub>	27.6894153	3.2384	42	E <sub>1g</sub>	12.1107593	0	78	E <sub>2g</sub>	7.09505964	0
13	E <sub>1u</sub>	27.6894153	3.2386	43	E <sub>1g</sub>	12.1107593	0	79	E <sub>2g</sub>	7.01163618	0
14	E <sub>1g</sub>	23.1468329	0	44	A <sub>2u</sub>	11.7981278	192.3288	80	E <sub>2g</sub>	7.01163618	0
15	E <sub>1g</sub>	23.1468329	0	45	A <sub>2g</sub>	11.0741072	0	81	B <sub>2u</sub>	6.83597544	0
16	A <sub>1g</sub>	22.1075224	0	46	A <sub>1u</sub>	10.7907109	0	82	E <sub>1u</sub>	6.77066064	1.4942
17	B <sub>2u</sub>	21.8765877	0	47	E <sub>1g</sub>	10.6879757	0	83	E <sub>1u</sub>	6.77066064	1.4941
18	E <sub>2g</sub>	21.1538499	0	48	E <sub>1g</sub>	10.6879757	0	84	A <sub>2g</sub>	6.60787099	0
19	E <sub>2g</sub>	21.1538499	0	49	E <sub>2u</sub>	10.5393755	0	85	B <sub>1u</sub>	6.59224726	0
20	A <sub>1u</sub>	19.8763211	0	50	E <sub>2u</sub>	10.5393755	0	86	A <sub>1g</sub>	6.35448932	0
21	E <sub>2u</sub>	19.0190089	0	51	B <sub>2g</sub>	10.4517908	0	87	E <sub>2g</sub>	6.30083521	0
22	E <sub>2u</sub>	19.0190089	0	52	E <sub>2g</sub>	10.3418619	0	88	E <sub>2g</sub>	6.30083521	0
23	B <sub>1u</sub>	18.7896828	0	53	E <sub>2g</sub>	10.3418619	0	89	E <sub>1u</sub>	6.2992348	12.1109
24	A <sub>2u</sub>	18.6925472	28.2844	54	A <sub>1g</sub>	9.96529047	0	90	E <sub>1u</sub>	6.2992348	12.1117
25	B <sub>2g</sub>	16.4914584	0	55	E <sub>1u</sub>	8.92372919	7.4894	91	A <sub>2g</sub>	3.29392677	0
26	A <sub>2g</sub>	16.1440355	0	56	E <sub>1u</sub>	8.92372919	7.4907	92	E <sub>1u</sub>	3.29304381	7.5751
27	E <sub>1g</sub>	15.6390195	0	57	B <sub>2u</sub>	8.79944182	0	93	E <sub>1u</sub>	3.29304381	7.5769
28	E <sub>1g</sub>	15.6390195	0	58	B <sub>1u</sub>	8.77254423	0	94	E <sub>2g</sub>	3.29138422	0
29	B <sub>1u</sub>	15.3660987	0	59	E <sub>2g</sub>	8.71591876	0	95	E <sub>2g</sub>	3.29138422	0
30	E <sub>2g</sub>	15.1289339	0	60	E <sub>2g</sub>	8.71591876	0	96	B <sub>1u</sub>	3.29065013	0
				61	B <sub>2u</sub>	8.55575688	0	97	B <sub>2u</sub>	3.27247243	0
				62	E <sub>1u</sub>	8.35950295	0.779	98	E <sub>2g</sub>	3.27133845	0
				63	E <sub>1u</sub>	8.35950295	0.7795	99	E <sub>2g</sub>	3.27133845	0
				64	A <sub>1g</sub>	8.30114047	0	100	E <sub>1u</sub>	3.26932595	133.2718
				65	E <sub>2g</sub>	8.27591916	0	101	E <sub>1u</sub>	3.26932595	133.2895
				66	E <sub>2g</sub>	8.27591916	0	102	A <sub>1g</sub>	3.26764374	0

Symmetry, A<sub>1g</sub>:A<sub>1g</sub> A<sub>2g</sub>:A<sub>2g</sub> B<sub>1g</sub>:B<sub>1g</sub> B<sub>2g</sub>:B<sub>2g</sub> E<sub>1g</sub>:E<sub>1g</sub> E<sub>2g</sub>:E<sub>2g</sub> A<sub>1u</sub>:A<sub>1u</sub> A<sub>2u</sub>:A<sub>2u</sub> B<sub>1u</sub>:B<sub>1u</sub> B<sub>2u</sub>:B<sub>2u</sub> E<sub>1u</sub>:E<sub>1u</sub> E<sub>2u</sub>:E<sub>2u</sub>

(Above wavelength are DFT calculated and corrected by scale factor 0.958 and red shift by 15cm<sup>-1</sup>.)

## Appendix 2. C<sub>23</sub>H<sub>12</sub><sup>++</sup> fundamental vibrations

Harmonic number	C2 point group symmetry	wavelength (μm)	IR intensity (km/mol)								
1	B	128.440089	4.5889	31	B	14.3209489	48.8426	67	B	7.93881251	49.4827
2	A	120.958215	1.3381	32	A	13.9463428	9.6893	68	B	7.87824296	24.0121
3	B	101.006008	11.8229	33	B	13.4751733	11.4881	69	A	7.82390005	289.2797
4	A	62.1307205	0.0878	34	A	13.4659461	12.0032	70	A	7.71224685	62.6043
5	B	56.3712692	55.1832	35	A	12.9848813	9.2307	71	B	7.57513734	258.571
6	A	45.7129869	8.376	36	B	12.8866774	80.717	72	B	7.44940841	36.8803
7	B	41.5036719	11.4499	37	A	12.5909407	0.2628	73	A	7.4406304	0.1248
8	A	36.2784414	0.2552	38	B	12.2823723	85.3515	74	B	7.36462829	58.0227
9	A	34.9079549	0.2215	39	A	12.1964302	20.7214	75	A	7.26920712	102.9819
10	B	33.9062235	3.1309	40	B	11.9792603	36.3086	76	B	7.26689949	23.4804
11	B	31.0090831	86.9236	41	A	11.8196108	0.7153	77	B	7.24181688	83.7932
12	A	29.0964620	11.6713	42	B	11.6879829	1.0484	78	A	7.09016378	3.7945
13	B	25.9762776	0.905	43	B	11.4444167	136.2236	79	A	7.02878645	15.203
14	A	23.7847460	0.003	44	B	11.1885463	23.0379	80	B	6.98309313	2.1444
15	B	23.4045730	2.1241	45	A	10.9410211	32.1274	81	B	6.86499217	13.7586
16	A	23.2859605	2.8943	46	B	10.7894572	11.7865	82	A	6.84221730	15.1946
17	B	22.1422764	46.4723	47	A	10.595496	15.8518	83	A	6.72288351	1.5501
18	A	21.4372883	1.1949	48	A	10.375279	7.64	84	A	6.62131864	19.7922
19	B	21.0467167	3.6327	49	B	10.3010348	0.8388	85	B	6.60255991	43.2698
20	A	20.3045203	1.3847	50	B	10.196156	15.6457	86	A	6.4851474	60.5678
21	A	19.4352599	13.3558	51	A	10.1780281	8.7556	87	B	6.46454552	239.7199
22	B	18.7795533	17.3062	52	B	10.0862667	0.0246	88	B	3.25254924	0.4922
23	A	18.2282356	0.31	53	A	10.0783465	10.0546	89	A	3.25190834	0.4489
24	B	17.8177725	8.1806	54	B	9.45675166	12.2548	90	B	3.25026212	2.2571
25	B	17.0906194	45.5637	55	A	9.37179293	30.0139	91	A	3.25020656	0.7123
26	A	16.1129599	1.2534	56	B	9.19611578	100.7882	92	B	3.23918786	2.7907
27	A	15.8663897	0.076	57	A	9.02729871	10.4829	93	A	3.2382037	2.6755
28	A	14.9911342	0.265	58	A	8.96936286	45.5088	94	B	3.23171955	7.6982
29	B	14.9337759	3.7441	59	B	8.95409808	27.1882	95	A	3.23169234	0.1246
30	B	14.4194092	7.1985	60	A	8.82668996	5.762	96	B	3.21464771	12.7718
				61	B	8.65430516	165.7545	97	A	3.21389777	0.1229
				62	A	8.3208072	103.2221	98	A	3.19430118	42.5184
				63	A	8.30433814	0.4494	99	B	3.19386244	12.9836
				64	B	8.27824912	65.8739				
				65	B	8.18188999	7.8531				
				66	A	7.97588222	0.1897				

### 6, VIBRATIONAL MODE ANALYSIS OF C<sub>23</sub>H<sub>12</sub><sup>++</sup>

Vibrational mode analysis using Gaussian09 package was summarized in Table 2, which was classified as follows,

(1) 3.19 μm (calculated and corrected value): C-H stretching mode at two pentagon sites.

(2) 6.46 μm: C-C stretching at all hexagon sites.

Calculated wavelength was longer than observed

one by 0.26 μm.

(3) 8.97-9.19 μm: Not identified in observed spectra

(4) 11.4-12.9 μm: C-H out-of-plane bending and C-C stretching

(5) 13.5 μm: C-H out-of-plane bending at pentagon site

(6) 14.3 μm: C-H out-of-plane bending at pentagons and C-C stretching.

These vibration mode features are almost similar to common PAH mode analysis on a review paper (see page 1028, Tielen; 2013)

## 7, CONCLUSION

In order to analyze vibrational mode of void induced coronene molecules, density functional theory was applied. Among them, di-cation  $C_{23}H_{12}^{++}$  is a possible carrier of the astronomically observed polycyclic aromatic hydrocarbon (PAH).

(1)Based on unrestricted density functional theory, multiple spin state analysis was done for neutral void coronene  $C_{23}H_{12}$ . Singlet spin state was most stable (lowest total energy).

(2)By the Jahn-Teller effect, there occurs serious molecular deformation. Point group  $D_{6h}$  of pure coronene transformed to  $C_2$  symmetry in  $C_{23}H_{12}$  having carbon two pentagons.

(3)Advanced singlet stable molecules were di-cation  $C_{23}H_{12}^{++}$  and di-anion  $C_{23}H_{12}^{--}$ . Molecular configuration was almost similar with neutral  $C_{23}H_{12}$ .

(4)Electric dipole moment of  $C_{23}H_{12}^{++}$  and  $C_{23}H_{12}^{--}$  show reversed direction each other with 1.19 and 2.63 Debye.

(5)Calculated infrared harmonic wavelength and relative peak height of  $C_{23}H_{12}^{++}$  show a very likeness to observed one of two astronomical sources of HD44179 and NGC7027. Observed emission peaks of 3.3, 6.2, 7.6, 7.8, 8.6, 11.2, 12.7, 13.5 and 14.3 $\mu$ m were compared well with single molecule  $C_{23}H_{12}^{++}$  calculated peaks of 3.2, 6.5, 7.6, 7.8, 8.7, 11.4, 12.9, 13.5, and 14.3 $\mu$ m.

(6)Harmonic vibrational mode analysis was done for  $C_{23}H_{12}^{++}$ . At wavelength 3.2  $\mu$ m, C-H stretching at pentagons was featured. From 6.4 to 8.7 $\mu$ m, C-C stretching mode was observed. In-plane-bending of C-H was in a range of 7.6-9.2 $\mu$ m. Both C-H out-of plane bending and C-C stretching were accompanied from 11.4 to 14.3 $\mu$ m.

## REFERENCES

- Armus, L., Charmandaris, V., Bernard-Salas, J., et al. 2007, *ApJ*, **656**, 148
- Bauschlicher, C. W., & Langhoff, S. R. 1997, *Spectrochim. Acta A*, **53**, 1225
- Bauschlicher, C. W., Peeters, E., & Allamandola, L. J. 2008, *ApJ*, **678**, 316
- Bauschlicher, C. W., Peeters, E., & Allamandola, L. J. 2009, *ApJ*, **697**, 1467
- Becke, A. D. 1993, *J. Chem. Phys.*, **98**, 5648
- Boersma, C., Bregman, J.D. & Allamandola, L. J. 2013, *ApJ*, **769**, 117
- Boersma, C., Bauschlicher, C. W., Ricca, A., et al. 2014, *ApJ Supplement Series*, **211**:8
- Boersma, C., Mattioda, A. L., Bauschlicher JR, C. W., et al. 2009, *ApJ*, **690**, 1208
- Cook, D. J., Schlemmer, S., Balucani, N., et al. 1998, *J. Phys. Chem.*, **102**, 1467
- de Frees, D. J., Miller, M. D., Talbi, D., Pauzat, F., & Ellinger, Y. 1993, *ApJ*, **408**, 530
- Engelbracht, C. W., Kundurthy, P., Gordon, K. D., et al. 2006, *ApJ*, **642**, L127
- Frisch, M. J., Pople, J. A., & Binkley, J. S. 1984, *J. Chem. Phys.*, **80**, 3265
- Frisch, M. J., Trucks, G.W., Schlegel, H. B., et al. 2009, Gaussian 09, Revision A.02 (Wallingford, CT: Gaussian, Inc.)
- Geballe, T. R., Tielens, A. G. G. M., Allamandola, L. J., Moorhouse, A., & Brand, P. W. J. L. 1989, *ApJ*, **341**, 278
- Hudgins, D. M., & Allamandola, L. J. 1999a, *ApJ*, **516**, L41
- Hudgins, D. M., & Allamandola, L. J. 1999b, *ApJ*, **513**, L69
- Kim, H.-S., Wagner, D. R., & Saykally, R. J. 2001, *Phys. Rev. Lett.*, **86**, 5691
- Langhoff, S. R. 1996, *J. Phys. Chem.*, **100**, 2819
- Mallocci, G., Joblin, C., & Mulas, G. 2007, *Chem. Phys.*, **332**, 353
- Meeus, G., Waters, L. B. F. M., Bouwman, J., et al. 2001, *A&A*, **365**, 476
- Moutou, C., Leger, A., & D'Hendecourt, L. 1996, *A&A*, **310**, 297
- Moutou, C., Sellgren, K., Verstraete, L., & L'eger, A. 1999, *A&A*, **347**, 949
- Ota, N., Gorjizadeh, N. & Kawazoe, Y., 2011, *Journal of Magnetics Society of Japan*, **35**, 414
- Ota, N. 2014a, arXiv org., **1408.6061**
- Ota, N. 2014b, arXiv org., **1412.0009**
- Oomens, J. 2011, in *In PAHs and the Universe: A Symposium to Celebrate the 25th Anniversary of the PAH Hypothesis*, EAS Publications Series, ed. A. G. G. M. Tielens & C. Joblin (Cambridge: Cambridge University Press), **46**, 61
- Oomens, J., Sartakov, B. G., Tielens, A. G. G. M., Meijer, G., & von Helden, G. 2001, *ApJ*, **560**, L99
- Oomens, J., Tielens, A. G. G. M., Sartakov, B. G., von Helden, G., & Meijer, G. 2003, *ApJ*, **591**, 968
- Pathak, A., & Rastogi, S. 2007, *Spectrochim. Acta A*, **67**, 898
- Peeters, E., Hony, S., van Kerckhoven, C., et al. 2002, *A&A*, **390**, 1089
- Piest, H., von Helden, G., & Meijer, G. 1999, *ApJ*, **520**, L75
- Regan, M. W., Thornley, M. D., Bendo, G. J., et al. 2004, *ApJS*, **154**, 204
- Ricca, A., Bauschlicher, C. W., Jr., Boersma, C., Tielens, A. & Allamandola, L. J. 2012, *ApJ*, **754**, 75
- Ricca, A., Bauschlicher, C. W., Jr., Mattioda, A. L., Boersma, C., & Allamandola, L. J. 2010, *ApJ*, **709**, 42
- Ricca, A., Bauschlicher, C. W., Jr., & Allamandola, L. J. 2011b, *ApJ*, **729**, 94
- Schlemmer, S., Cook, D. J., Harrison, J. A., et al. 1994, *Science*, **265**, 1686
- Sellgren, K., Uchida, K. I., & Werner, M. W. 2007, *ApJ*, **659**, 1338
- Smith, J. D. T., Draine, B. T., Dale, D. A., et al. 2007, *ApJ*, **656**, 770
- Szczepanski, J., & Vala, M. 1993a, *ApJ*, **414**, 646
- Phys.*, **14**, 2381
- Tielens, A. G. G. M. 2013, *Rev. Mod. Phys.*, **85**, 1021
- Verstraete, L., Puget, J. L., Falgarone, E., et al. 1996, *A&A*, **315**, L337

Submitted Jan. 8, 2015 by Norio Ota